Catalysis Today 146 (2009) 132–140

Contents lists available at ScienceDirect

Catalysis Today

journal homepage: www.elsevier.com/locate/cattod

Nanocomposite catalysts for internal steam reforming of methane and biofuels in solid oxide fuel cells: Design and performance

Vladislav Sadykov [a,*], Natalia Mezentseva [a], Galina Alikina [a], Rimma Bunina [a], Vladimir Pelipenko [a], Anton Lukashevich [a], Sergei Tikhov [a], Vladimir Usoltsev [a], Zakhar Vostrikov [a], Oleg Bobrenok [b], Alevtina Smirnova [c], Julian Ross [d], Oleg Smorygo [e], Bert Rietveld [f]

[a] Boreskov Institute of Catalysis, Novosibirsk, 630090, Russia
[b] Institute of Thermal Physics, Novosibirsk, 630090, Russia
[c] Connecticut Global Fuel Cell Center, UConn, Storrs, CT, USA
[d] Centre of Environmental Research, University of Limerick, Limerick, Ireland
[e] Powder Metallurgy Institute, Minsk, 220005, Belarus
[f] Energy Research Center of the Netherlands, Petten, The Netherlands

ARTICLE INFO

Article history:
Available online 29 March 2009

Keywords:
Composites
Ni–YSZ (ScCeSZ)
Doped ceria–zirconia oxides
Complex chromites
Ru
Pt
Pd
Steam reforming
CH_4
Ethanol
Acetone

ABSTRACT

Nanocomposite catalysts comprised Ni particles embedded into the complex oxide matrix comprised Y- or Sc-stabilized zirconia (YSZ, ScCeSZ) combined with doped ceria–zirconia oxides or La–Pr–Mn–Cr–O perovskite and promoted by Pt, Pd or Ru were synthesized via different routes (impregnation of YSZ or NiO/YSZ composites with different precursors, one-pot Pechini procedure). Both composition and preparation procedure determining degree of interaction between components of composites were found to strongly affect performance of nanocomposites in steam reforming of methane at short contact times as well as their stability to coking in stoichiometric feeds. Temperature-programmed reduction of composites by CH_4 followed by temperature-programmed oxidation by H_2O revealed more efficient dissociation of CH_4 on promoted composites yielding loose surface CH_x species more easily removed by water as compared with unpromoted composites. Best active components highly active and stable to coking were supported as thin layers on different substrates (Ni/YSZ anode platelets, refractory dense/porous metal alloys, cermet or corundum monolithic carriers). These structured catalysts demonstrated high efficiency and stability in the reactions of steam reforming of methane and oxygenates (ethanol, acetone) in pilot-scale reactors.

1. Introduction

Design of catalytic materials for internal steam reforming of methane in the intermediate temperature solid oxide fuel cells (IT SOFC) able to efficiently operate in feeds with a small (if any) excess of steam without coking represents important but demanding problem [1]. State-of-the-art $Ni/Y_2O_3–ZrO_2$ (Ni/YSZ) cermet anodes of solid oxide fuel cells have excellent catalytic properties and stability in the oxidation of hydrogen fuel at SOFC operation conditions [2]. However, the lack of a hydrogen infrastructure and the unsolved hydrogen storage problem have initiated the research aimed at direct utilization of natural gas, which represents one of the key aspects of SOFC technology. Internal steam reforming (SR) is the most promising concept in using the natural gas as a fuel [3,4]. In this case, the reaction takes place directly in the anode compartment, allowing within a stack a better management of heat produced by the exothermic electrochemical oxidation and consumed by the endothermic reforming reaction. For solid oxide fuel cells, an attractive option is direct internal reforming of bio-fuels on catalytically active anodes [5]. Unfortunately, with the Ni/YSZ cermet, coking occurs leading to the deterioration of anode performance [2,4]. Ni/YSZ cermet anodes can be used in hydrocarbons or oxygenates reforming only if the excess steam is present to suppress the carbon deposition. In this case, the overall electrical efficiency of the cell decreases due to the energy consumption for the excess water evaporation [3,4]. Hence, development of robust anode materials with a high and stable catalytic activity in the internal steam reforming of hydrocarbons/oxygenates in feeds with a small excess of steam is vital for design of SOFC.

The most promising approach to design of inexpensive catalytic materials possessing a high activity and coking stability in CH_4

* Corresponding author at: Boreskov Institute of Catalysis, Heterogeneous Catalysis, pr. Lavrentieva, 5, Novosibirsk, 630090, Russia. Tel.: +7 383 330 87 63; fax: +7 383 330 80 56.
E-mail address: sadykov@catalysis.ru (V. Sadykov).

0920-5861/$ – see front matter © 2009 Elsevier B.V. All rights reserved.
doi:10.1016/j.cattod.2009.02.035

steam reforming in the middle-temperature range is to promote traditional cermets such as Ni/YSZ- or Ni/Sc–Ce-stabilized zirconia (Ni/ScCeSZ) by fluorite-like (doped ceria–zirconia) or perovskite-like (mixed chromates–manganites) oxides along with small (~1 wt.%) amounts of precious metals (Pt, Pd, Ru) [6–10]. In these systems, Ni and/or precious metals are responsible for activation of CH_4 molecules, while oxide components provide activation of water molecules and transfer of hydroxyls and/or hydroxocarbonate/oxygen species to the metal particles–oxide interface where they interact with activated C–H–O species producing syngas [6,7].

This paper summarizes experimental results on the catalytic properties of composite materials in methane SR in regard of the nature and content of a precious metal, a type of the oxide additive, the nature of doped zirconia electrolyte and the method of promoted composites preparation presented in part in earlier publications [8–11]. Detailed structural studies revealing pronounced interaction between the components of composites controlling their catalytic properties and reactivity were also reported earlier [8–11] and will be here referred to only in the extent required for explanation of the specific features of these systems performance. CH_4 temperature-programmed reduction (TPR) experiments followed by H_2O temperature-programmed oxidation (TPO) were used here for the first time to elucidate effects of interaction between the components of composites on the ability of surface sites to efficiently dissociate CH_4 molecules without forming dense graphite-like layers or whiskers and catalyze oxidation of surface polymerized CH_x species into syngas.

The best compositions supported as porous strongly adhering layers on anode platelets, nonporous (Crofer interconnects) or porous (Ni–Al foam) alloy substrates, corundum or cermet monolithic substrates [12] were tested in the reactions of methane and oxygenates (ethanol, acetone) steam reforming in pilot-scale installations.

2. Experimental

Catalysts prepared and studied in this work were based upon next types of composites:

(1) Composite **I** (specific surface area 11 m^2/g) comprised 60 wt.% NiO + 40 wt.% YSZ was prepared by mixing and ball milling of industrial sources as described elsewhere [8,9]. This composite was promoted by supporting 10 wt.% of fluorite-like ($Ce_{0.5}Zr_{0.5}O_{2-x}$, $Pr_{0.3}Ce_{0.35}Zr_{0.35}O_2$, $La_{0.3}Ce_{0.35}Zr_{0.35}O_2$) or perovskite-like ($La_{0.8}Pr_{0.2}Mn_{0.2}Cr_{0.8}O_3$) oxides by impregnation with water solutions of corresponding polyester citric acid–ethylene glycol precursors followed by drying and calcination in air at 700 °C for 4 h.

(2) Composite **II** (specific surface area 23 m^2/g) comprised 10 wt.% $La_{0.8}Pr_{0.2}Mn_{0.2}Cr_{0.8}O_3$ + 55 wt.% NiO + 35 wt.% ScCeSZ was prepared using powdered $Sc_{0.1}Ce_{0.01}Zr_{0.89}O_{2-y}$ electrolyte synthesized by co-precipitation as described elsewhere [13]. ScCeSZ powder was first dispersed in the water solution of Ni nitrate and polyester citric acid–ethylene glycol polymeric precursor of perovskite following so-called one-pot synthesis routine [10]. After evaporation, formed solid residue was decomposed in air at 500 °C and then calcined at 700 °C for 4 h.

(3) Composite **III** (specific surface area 9 m^2/g) comprised 60 wt.% NiO + 40 wt.% YSZ was prepared by impregnation of powdered $Y_{0.08}Zr_{0.92}O_{2-y}$ (Russian source) with Ni nitrate solution followed by drying overnight in air at 90 °C with subsequent calcination at 800 °C. After regrinding, the composite **III** was loaded with 10 wt.% fluorite-like oxides ($Pr_xCe_yZr_zO_2$, $La_qPr_{x-}Ce_yZr_zO_2$, $Sm_qPr_xCe_yZr_zO_2$, where $y = 0.35, 0.05$; $z = 0.35, 0.25, 0.2$; $x = 0.15–0.3$; $q = 0.15$) by impregnation with respective mixed nitrates solutions followed by drying and calcination at 800 °C [10].

(4) Composite **IV** (specific surface area 28 m^2/g) comprised 10 wt.% $Pr_{0.15}La_{0.15}Ce_{0.35}Zr_{0.35}O_2$ + 55 wt.% NiO + 35 wt.% YSZ (Russian source) was prepared by the one-pot Pechini procedure similar to that used for preparation of composite **II**.

Pt, Pd or Ru (0.3–1.4 wt.%) were supported on composites **I–III** by the incipient wetness impregnation with $PdCl_2$, H_2PtCl_6 or $RuCl_3$ solutions followed by drying and calcinations at 800 °C for 2 h.

For supporting thin layers of nanocomposites, NiO/YSZ green anode plates (manufactured and supplied by FRZ Jülich, Germany, or ECN, Netherlands, covered on one side by catalytically inactive dense YSZ layer), Crofer interconnects and NiAl foam substrates were used. Open-cell nickel foams were manufactured by the nickel electroplating of the polyurethane foam samples (thickness 5 mm, the cell density 60 ppi) followed by sintering in the dissociated ammonia atmosphere at 1100 °C for 1 h. The foam samples were then deformed by a uniaxial compression to 1 mm thickness modifying the cell morphology and decreasing porosity from 95.5% to 60–80%. Deformed foams were subjected to the pack aluminizing and then annealed at 1000 °C for 1 h under air to form a thin α-alumina layer over the foam cell walls for a better adhesion of catalytic layers.

Crofer interconnect substrates were precovered by a dense corundum sublayer through the blast dusting procedure [11,14].

Characteristics of thin-wall honeycomb monolithic corundum substrates or microchannel Cr–Al composite substrates used for supporting nanocomposite active components were described in details elsewhere [12,15,16].

Composite powders comprised 10 wt.% complex oxide promoter +55 wt.% NiO + 35 wt.% YSZ (Russian source) synthesized via one-pot Pechini route (vide supra) were ultrasonically dispersed in isopropyl alcohol with addition of polyvinyl butyral as a binder to make a slurry. Thin layers of composites were supported on substrates using these slurries and slip casting or painting procedures followed by drying and calcination at 1100 °C after each supporting step until loading of 4–7 wt.% was achieved. Ru or Pt (loading in the range of 0.5–1.0 wt.% as related to the weight of composite) was supported by the incipient wetness impregnation followed by drying and calcination under air at 800 °C.

SEM images of Ni–Al foam and composite layers on substrates were made with a JSM-6460 LV (Jeol) microscope.

Experiments for temperature-programmed reduction of samples by CH_4 (1% CH_4 in He feed) and their subsequent temperature-programmed oxidation by H_2O (1% H_2O in He feed) were carried out in flow installations equipped with quartz reactors, GC and PEM-2M gas analyzers under the temperature ramp of 5°/min up to 880 °C with the isothermal plateau at 880 °C for 70 min [9–11]. After CH_4 TPR run, samples were rapidly cooled in the flow of He to room temperature, then He stream was switched to 1% H_2O in He flow and the temperature ramp was repeated.

The steady-state activity of catalysts (0.25–0.5 mm fraction of powdered samples or platelets with a typical size 1 cm × 2 cm) in CH_4 SR was estimated in He- or Ar-diluted feeds with CH_4 concentration up to 20% and steam/methane ratio 1–3 using specially designed flow quartz reactors. The contact time was varied in the range of 10–70 ms. GC and PEM-2M gas analyzers were used for analysis of reagents and products [9–11]. Before reaction, samples were pretreated in O_2 at 500 °C for 1 h. Typically, experiments were started at 750 °C to reduce samples *in situ* by stoichiometric CH_4/H_2O feed with subsequent cycling of temperature in the studied range and keeping a sample at least 1 h at each temperature to obtain reproducible steady-state results.

Catalytic performance of monolithic catalysts with nanocomposite active components in the reactions of steam/autothermal

reforming of ethanol or acetone was studied in the stainless steel flow reactors equipped with external heating coils [12,14,16] using a pilot-scale installation. A liquid mixture of water and oxygenates was supplied by a pump and sprayed via a nozzle into a specially designed monolithic honeycomb evaporation/mixing unit heated by passing the electric current. Reagents and products concentrations were analyzed by GC.

3. Results and discussion

3.1. Summary of phase composition and microstructure data [8–11,13]

Detailed studies of composites structural and microstructural characteristics by X-ray diffraction (XRD) and high resolution transmission electron microscopy (TEM) with elemental analysis (EDX) confirmed presence of perovskites-like phase (PDF#89-8771) or fluorite-like doped ceria–zirconia phase (PDF#02-1334) both before and after contact with the reaction feed at operation temperatures [8–11,13]. Pronounced interaction between all phases of composites leading to redistribution of elements, particles intergrowth and decoration of the surface layers of one phase (i.e., NiO) by clusters of another one (i.e., a complex oxide promoter or precious metals) was reliably established by TEM with EDX. This interaction was also reflected in variation of samples reactivity (mainly, NiO phase) as studied by the temperature-programmed reduction with H_2 or CH_4 [8–11,13]. After contact with the reaction feed, reflections of NiO phase (PDF# 02-1334) disappear completely while those of Ni^0 (PDF#04-850) emerge [9]. After reaction, particles of complex oxides remain in a close contact with Ni^0 particles. This provides developed Ni^0–complex oxide interface considered to be important for the efficient transformation of activated CH_x fragments into syngas, thus preventing coke formation [6,7].

3.2. Catalytic properties of dispersed promoted composites in methane steam reforming

Composites with fluorite-like oxide additives. In the stoichiometric feed, composites **I** and **III** possess noticeable activity starting from ~700 °C [8–11], while at temperatures exceeding 800 °C their activity declines due to coking. Supporting complex ceria–zirconia oxides increases catalysts performance at temperatures exceeding 600 °C and stabilizes it at high temperatures (Fig. 1, Table 1) apparently due to hampering of coking. Some samples based upon fluorite oxides promoted composite **III** remain inactive at 650 °C (Table 1), while composite **IV** demonstrates a good performance starting already from 550 °C (Fig. 1). This can be explained both by a higher specific surface area of composite **IV** as well as by a higher degree of interaction between components of this composite provided by one-pot Pechini route of synthesis, and, hence, stabilization of small active Ni clusters on the surface of oxidic components of composite [8–11].

For the stoichiometric feed, Pd as co-promoter further increases performance of ceria–zirconia promoted composite **I** (Table 1) making it highly active even at temperatures below 600 °C [8,9]. Pt as co-promoter also ensures a high activity in the middle-temperature range (Fig. 1, Table 1). Indeed, at 650 °C, efficient first-order rate constants estimated for the plug-flow reactor are as high as 30–40 s^{-1} [8–11]. Hence, more efficient activation of CH_4 molecules on Pt or Pd clusters [17] allows to increase the overall performance of Ni-containing catalysts in the IT range, while dispersed fluorite-like oxide promoter apparently plays the major role in activation of water molecules and transfer of activated oxygen-containing species (hydroxyls, hydroxocarbonates) to the sites where activated CH_x species are located, thus preventing formation of coke.

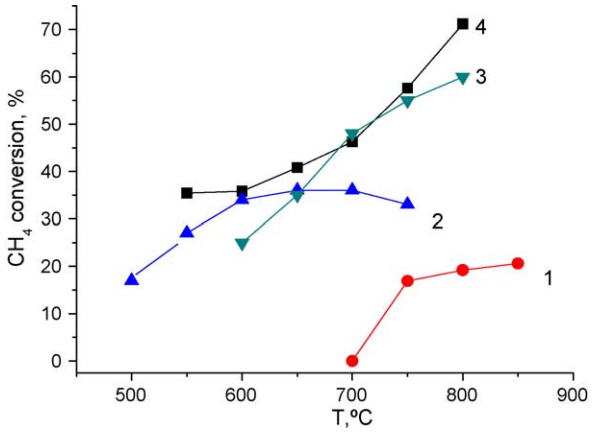

Fig. 1. Temperature dependence of CH_4 conversion in stoichiometric steam/methane feed for different composites: 1, 10 wt.% $Pr_{0.3}Ce_{0.35}Zr_{0.35}O_2$/composite **III**; 2, 1.3 wt.% Ru/10 wt.% $Pr_{0.15}La_{0.15}Ce_{0.35}Zr_{0.35}O_2$/composite **III**; 3, 0.3 wt.% Pt/10 wt.% $Pr_{0.3}Ce_{0.35}Zr_{0.35}O_2$/composite **I**; 4, composite **IV**. Contact time 10 ms, 8% CH_4 + 8% H_2O in Ar.

The performance of samples co-promoted with Pt and fluorite-like oxides tends to increase in feeds with the excess of steam (Table 1). This is important from the practical point of view since in real SOFC operation conditions, the oxygen ions transfer through the cell increases the overall content of oxidants within the porous composite anode. The increase of steam content in the feed increases the rate of activated hydrocarbons species transformation into syngas, thus preventing the surface coking and ensuring a high performance of composite co-promoted with Pt and fluorite-like oxide. For Pt as a co-promoter, the effect of the steam excess in feed strongly depends on the exact chemical composition of the oxide additive. Thus, for sample co-promoted with La–Ce–Zr–O oxide, the effect of the steam excess is small, while for combination of Pt with Pr–Ce–Zr–O oxide additive, this effect is well pronounced (Table 1).

Note also that for Pt-supported fluorite-like oxides without Ni addition (characterized in details in our previous publications [18–20]), performance is independent upon the water excess (Table 1).

Table 1
Values of CH_4 conversion for CH_4 SR at 650 °C on composites promoted with fluorite/perovskite-like oxides and Pt, Pd or Ru. 10 ms contact time, O_2 pretreatment; 1:1 feed (8% CH_4 + 8% H_2O in He) and 1:3 feed (8% CH_4 + 24% H_2O in He).

Composition	CH_4 conversion, %	
CH_4:H_2O	1:1	1:3
$Ce_{0.5}Zr_{0.5}O_2$/composite **I**	23	
1.4 wt.% Pt/$La_{0.3}Ce_{0.35}Zr_{0.35}O_2$	15	14
1.4 wt.% Pt/$Pr_{0.05}Ce_{0.45}Zr_{0.45}O_2$	35	
1.4 wt.% Pt/$Pr_{0.3}Ce_{0.35}Zr_{0.35}O_2$	22	
0.3 wt.% Pd/$Ce_{0.5}Zr_{0.5}O_2$/composite **I**	43	0
0.3 wt.% Pt/$La_{0.3}Ce_{0.35}Zr_{0.35}O_2$/composite **I**	30	26
0.3 wt.% Pt/$Pr_{0.3}Ce_{0.35}Zr_{0.35}O_2$/composite **I**	35	50
1.03 wt.% Pt/$Pr_{0.3}Ce_{0.35}Zr_{0.35}O_2$/composite **I**	0	52
0.5 wt.% Ru/$Pr_{0.3}Ce_{0.35}Zr_{0.35}O_2$/composite **I**	12	24
Composite **II**	1	
1 wt.% Ru/composite **II**	33	58
0.3 wt.% Ru/composite **II**	40	32
LaMnCrPr/composite **I**	20	
0.3 wt.% Pd/LaMnCrPr/composite **I**	26	12
1 wt.% Ru/LaMnCrPr/composite **I**	70	
$Pr_{0.3}Ce_{0.35}Zr_{0.35}O_2$/composite **III**	0	
1 wt.% Ru/$Pr_{0.3}Ce_{0.35}Zr_{0.35}O_2$/composite **III**	32	
1 wt.% Ru/$Pr_{0.15}La_{0.15}Ce_{0.35}Zr_{0.35}O_2$/composite **III**	36	
1 wt.% Ru/$Pr_{0.15}Sm_{0.15}Ce_{0.5}Zr_{0.2}O_2$/composite **III**	19	
Composite **IV**	40	

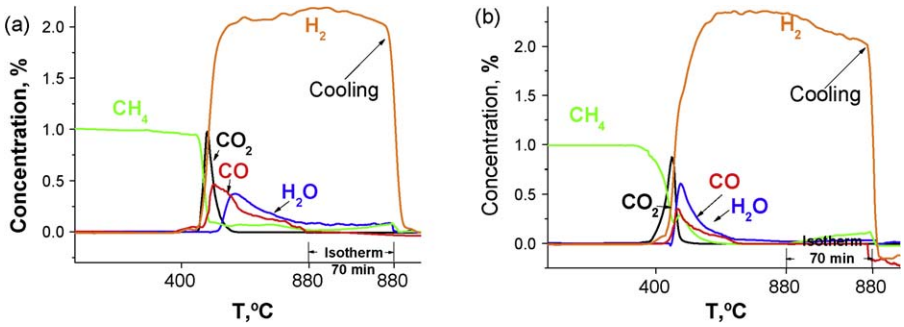

Fig. 2. CH_4 TPR curves for composite **III** (a) and 1.4 wt.% $Pt/Pr_{0.15}Sm_{0.15}Ce_{0.5}Zr_{0.2}O_2$/composite **III** sample (b).

A non-additive increase of performance due to supporting Pt along with fluorite-like oxides on Ni-containing composite (a synergetic effect) is thus apparent.

To clarify further the reason of this synergetic action of Pt and Ni, the temperature-programmed experiments have been carried out (Figs. 2–4). As follows from these results, co-promoting a composite by a fluorite-like oxide and Pt facilitates both the surface and bulk reduction (Fig. 2). This clearly correlates with easier (starting at lower temperatures) reduction of Pt-promoted doped ceria–zirconia oxide (Fig. 3). For all samples, the hydrogen evolution due to CH_4 dissociation (and, hence, carbon deposition on the surface) continues even after their complete reduction when CO and CO_2 evolution is stopped. For promoted reduced composites, their temperature-programmed oxidation (accompanied by hydrogen evolution) as well as oxidation of deposited carbon species (accompanied by CO_2, CO and H_2 evolution) starts earlier and proceeds faster (Fig. 4). Note that for Pt-supported doped ceria–zirconia sample oxidation of deposited carbonaceous species starts even earlier (Fig. 3), but continues for higher temperatures that for promoted composite (Fig. 3). This clearly demonstrates involvement of Ni surface atoms together with Pt in gasification of the surface coke which explains observed non-additive performance of promoted composites. Another new feature revealed in these experiments is evolution of CH_4 (or, in general, hydrocarbons) in the process of H_2O TPO of reduced and coked promoted composite (Fig. 3). This supports hypothesis that complex oxide promoters make deposited coke species less dense and, perhaps, containing a bigger fraction of hydrogen atoms [11]. As the result, they are more easily cracked by interaction with the surface hydroxyls yielding hydrocarbons.

For Pd supported on a composite promoted by ceria–zirconia, the increase of steam content in the feed suppresses the low-temperature performance (Table 1), which could be explained by stabilization of oxidized Pd species by fluorite-like oxide [8–11]. Here the main role is played by a higher stability of Pd oxidic forms (perhaps, some surface phases including both Pd and Ce cations) as compared with those of Pt. A lower ability of oxidized Pd species to activate methane is thus responsible for a low activity in feeds with the steam excess.

For Ru as a co-promoter of composite **I** in combination with the fluorite-like oxides, the excess of steam also positively affects the low-temperature performance (Table 1). However, this perfor-

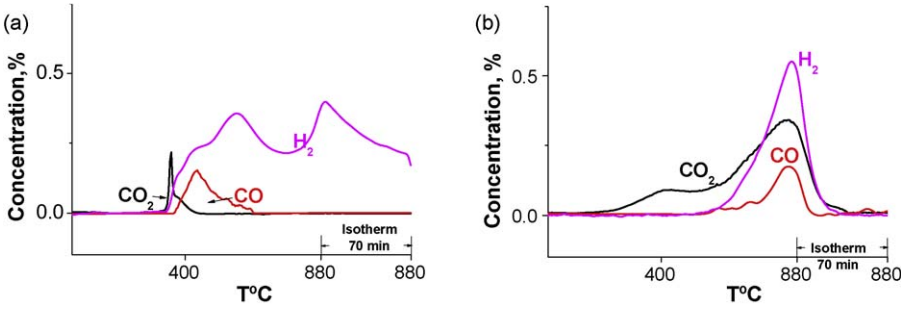

Fig. 3. CH_4 TPR (a) and subsequent H_2O TPO (b) experiments for 1.4 wt.% $Pt/Pr_{0.15}Sm_{0.15}Ce_{0.5}Zr_{0.2}O_2$ sample.

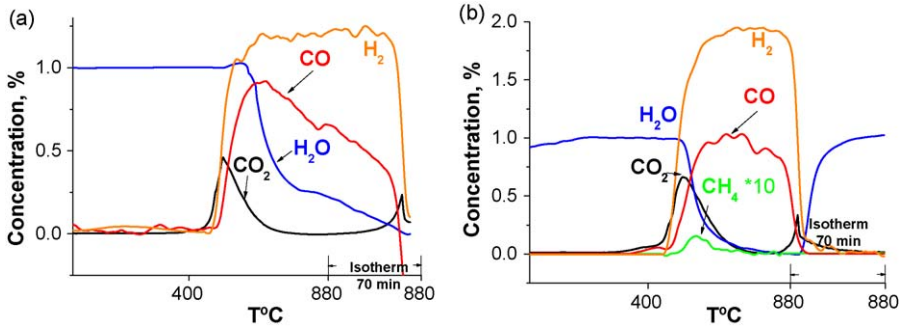

Fig. 4. Temperature-programmed oxidation by H_2O of reduced and coked composite **III** (a) and 1.4 wt.% $Pt/Pr_{0.15}Sm_{0.15}Ce_{0.5}Zr_{0.2}O_2$/composite **III** (b) samples after CH_4 TPR experiments (see Fig. 2).

mance is lower than for Pt-containing samples, so Pt is more efficient co-promoter than Ru in combination with complex fluorite-like oxides. This can be explained by a higher efficiency of Pt in activation of methane [17].

When Pt or Pd is supported on Ni/YSZ composite without oxide additives, methane conversion is not improved (not shown for brevity). This suggests that namely combination of precious metals with oxide promoters helps to provide enhanced activity of composites in the intermediate temperature range. Due to a low content of supported precious metals, their effect can be assigned to modification of some specific defect centers of Ni particles. This suggestion agrees with a high performance of composite **IY** prepared via a specific synthesis procedure (vide supra) even without promotion by precious metals.

Composites with perovskite-like oxide additives. Ni/ScCeSZ cermet without oxide promoters was not able to provide a steady-state performance in the methane SR in stoichiometric feeds due to very fast coking leading finally to the reactor plugging [8,9]. After reduction by H_2, composite **II** comprised Ni/ScCeSZ cermet promoted by perovskite-like oxide demonstrates a reasonably high and stable activity at temperatures exceeding 650 °C [9]. Similarly, promotion of composite **I** by perovskite oxide allows to obtain a reasonable performance in methane steam reforming even at 650 °C (Table 1). By itself, La–Pr–Mn–Cr–O perovskite is inactive in SR of methane. However, incorporation of Ni cations into the lattice of such perovskite provides a reasonable level of activity in methane steam reforming [21]. Hence, observed high and stable activity of perovskite-promoted composites in CH_4 SR in stoichiometric feed can be explained by partial dissolution of NiO in the acidic polyester solution at the preparation stage. At subsequent calcination, Ni-containing perovskite is formed. Under contact with reducing reaction media, small highly reactive Ni clusters are segregated on the surface of perovskite oxide being stabilized by interaction with this matrix stable in reducing conditions. In addition, the surface of big NiO particles in non-reduced composite is covered by the perovskite layers [9]. Hence, big Ni^0 particles generated due to NiO reduction in the reaction media are decorated by perovskite-like oxidic species. A high efficiency of these species and/or separate perovskite particles in activation of steam and carbon dioxide facilitates gasification of CH_x species produced by methane activation on Ni, thus preventing coking. This level of high-temperature activity for perovskite-promoted composite **I** (Table 1) is close to that provided by ceria–zirconia oxide promoter. Hence, similar factors affecting surface properties of Ni particles in promoted composites as well as enhanced activation of water and/or CO_2 molecules on the surface sites of oxide additives could operate in the case of both types of oxide promoters ensuring high and stable performance of composites in methane SR in stoichiometric feeds, especially at rather high (>700 °C) temperatures.

The increase of steam/methane ratio from 1 to 3 was found to decrease the high-temperature performance of perovskite-promoted composites [9]. This can be assigned to partial oxidation of Ni surface atoms contacting with perovskite species/particles and their stabilization as less active perovskites-like fragments.

Co-promotion of composites with perovskite-like oxide and Ru allowed to achieve a high level of middle-temperature activity in feeds with different steam/methane ratios (Table 1, Fig. 1). For composite **II**, the increase of Ru content from 0.3 to 1 wt.% decreases activity in the stoichiometric feed and increases it in the feed with the excess of steam (Table 1). This behavior can be explained by a higher rate of CH_4 activation on the surface of sample with a higher Ru content, thus leading to deactivation due to coking in stoichiometric feed. In a feed with the excess of steam, enhanced rate of activated CH_x species gasification prevents coking and provides a higher performance of sample with a higher Ru content due to a higher rate of CH_4 activation. Similar features observed for composite **I** co-promoted with fluorite-like oxide and Pt (Table 1) agree with this explanations of the precious metal content and feed composition effects.

Table 1 compares conversion of CH_4 at 650 °C for composites with two different electrolytes YSZ and ScCeSZ promoted by perovskite and precious metals. Perovskite as a promoter apparently ensures a higher activity at intermediate temperatures for YSZ-containing composite **I** despite a higher specific surface area and dispersion of nickel in ScCeSZ-based composite **II**. In the stoichiometric feed, combination of Ru and perovskite also ensures a higher activity of YSZ-containing samples. Hence, in general, catalysts containing YSZ electrolyte have a higher level of activity in steam reforming of methane in stoichiometric feeds than those containing ScCeSZ. In the case of composites containing YSZ, Pd was found to be less efficient promoter than Ru.

When comparing two series of samples co-promoted with precious metals and either fluorite-like or perovskite-like oxides (Table 1), the middle-temperature performance of the best samples of both series is comparable. For samples promoted with perovskite-like oxide, the highest activity is provided by supporting Ru, while for samples with fluorite-like oxide additives, the highest performance is observed after loading Pt. Hence, these two types of systems can be considered as promising for the practical application. In general, a better performance is provided by YSZ-containing catalysts. Though more detailed studies are required for elucidating the exact role played by the rare-earth cations (Sc, Y) in determining catalytic properties of these very complex materials, it is clear that observed trends are not determined by the oxygen mobility in doped zirconia particles which is higher for ScCeSZ [13].

Hence, the most efficient promoter for Ni/YSZ-based composite catalyst is Pr-doped ceria–zirconia in combination with Pt. Since Pt is more expensive than Ru, the latter was also used as a co-promoter in combination with either perovskite or fluorite oxide when supporting thin layers of NiO + YSZ-based nanocomposites on different substrates.

As far as the preparation procedures are concerned, one-pot Pechini route apparently provides the highest activity of promoted composites, at least, for systems with complex fluorite-like oxide additives. Hence, this method was selected as a basic one for preparation of dispersed promoted composites for subsequent supporting on different substrates.

3.3. Catalytic performance of small structural pieces of Ni–Al foams, interconnects and Ni/YSZ anode substrates with supported nanocomposite layers in CH_4 steam reforming

Typical morphology of compressed foam Ni–Al alloy substrate before and after supporting promoted composite materials is shown in Fig. 5. Applied supporting procedure ensured uniform filling of substrate macropores by porous nanocomposite.

Fig. 6 compares methane conversions in stoichiometric steam/methane feed for different plate-like structural elements with supported layers of nanocomposite containing fluorite-like oxide promoter and Ru. While at temperatures below 550 °C Ni/YSZ anode substrate is not active by itself, supporting composite layers on all substrates provides a reasonable activity in the low-temperature range. Basically, activity of these layers on different substrates is comparable, which agrees with a high intrinsic activity of nanocomposite active components (vide supra). This allows to use these structural elements for efficient in-cell steam reforming of methane to provide required heat management. A rather high activity of unpromoted FRZ Jülich anode platelet at temperatures exceeding 600 °C is worth noting as well.

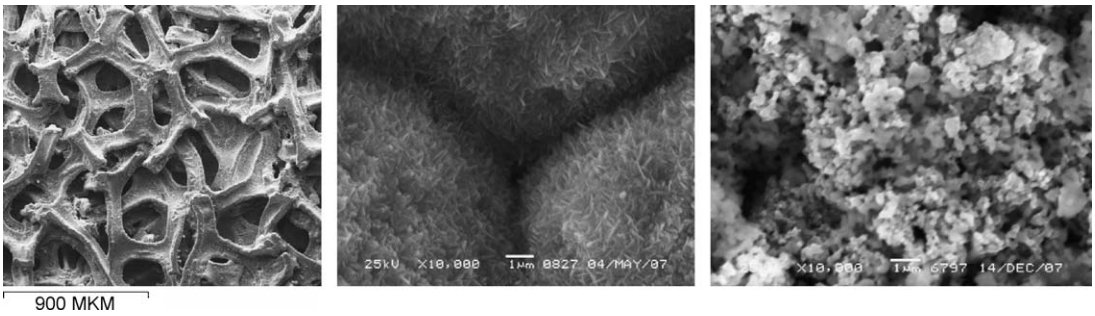

Fig. 5. Typical SEM images of initial porous foam-like Ni–Al substrate (a), a layer of needle-like corundum particles segregated on the Ni–Al alloy surface after high-temperature oxidation (b) and porous layer of composite filling macropores of foam substrate (c).

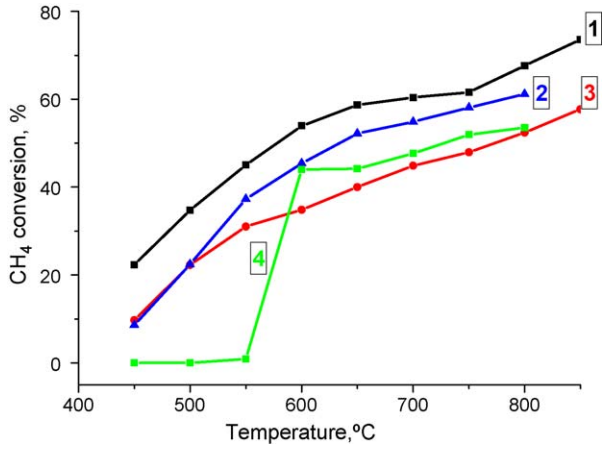

Fig. 6. Performance of nanocomposite 1 wt.% $Ru/Pr_{0.3}Ce_{0.35}Zr_{0.35}O_2$/Ni/YSZ layers on different substrates (1, Ni/YSZ platelet; 2, foam Ni–Al; 3, Crofer interconnect) and unpromoted Ni/YSZ anode platelet (4). 8% CH_4 + 8% H_2O in He, contact time 25 ms.

When nanocomposite layers supported on different substrates contain as co-promoters Ru and perovskite-like oxide, performance is better than for combination of Ru and fluorite-like oxide (Fig. 7), following a similar trend for powdered samples (vide supra).

Combination of Pt with fluorite-like oxide as co-promoters in supported nanocomposite layers on different substrates also provides a high and stable activity in methane steam reforming even in feeds with a higher (20%) concentration of methane close to realistic compositions (Fig. 8). In this case, close performance of supported nanocomposite layers on different substrates is observed as well.

Comparable or even better performance at shorter contact times was observed for nanocomposite layers covering one side of porous ECN anode substrates (Fig. 9). In this case, porosity of a substrate seems to play a positive role. A better performance was obtained for composite layers containing complex perovskite additive and Ru as co-promoters.

Stability tests (up to 35 h time-on-stream) for the unpromoted and nanocomposite covered FRZ Jülich anode platelet (Fig. 10) revealed a slow decline of unpromoted anode performance, while activity of promoted platelet is more stable.

As follows from both optical and SEM images after stability tests (Fig. 11), supported nanocomposite layer retains its integrity without any cracks or detachment from the underlying anode substrate despite transformation of NiO into Ni in composite as well as in the anode substrate in the reaction conditions. This is provided by a close composition of both substrate and supported layers ensuring matching of chemical and thermal coefficients of shrinkage/expansion. Developed porosity of supported layers helps to avoid diffusion limitations for rather fast CH_4 SR reaction.

In real conditions of SOFC operation under load, the oxygen transfer from the cathode to the anode side results in increasing the local oxygen chemical potential on the anode/gas phase interface which might affect performance of anode-supported composite catalytic layers in steam reforming of methane due to a partial oxidation of Ni/precious metals. In fact, in our experiments this effect was modeled by increasing H_2O content in the feed (vide supra). Based upon these results, Pd-promoted composites

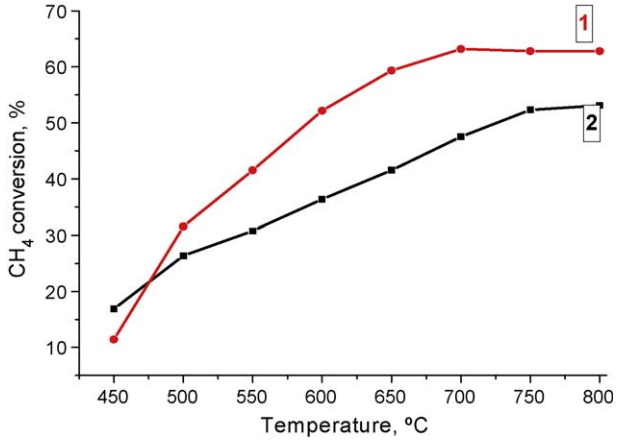

Fig. 7. Temperature dependence of CH_4 conversion for 0.5 wt.% $Ru/La_{0.8}Pr_{0.2}Mn_{0.2}Cr_{0.8}O_3$/Ni/YSZ (1) and 0.5 wt.% $Ru/Pr_{0.3}Ce_{0.35}Zr_{0.35}O_2$/Ni/YSZ (2) layers on thick (2 mm) planar FRZ Jülich anode substrate. 8% CH_4 + 8% H_2O in He, contact time 25 ms.

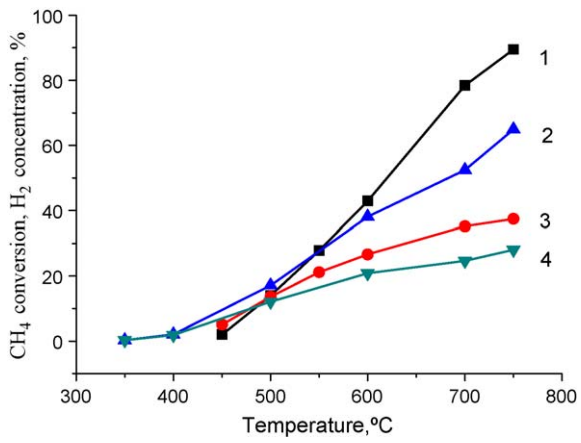

Fig. 8. Conversion of CH_4 (1, 2) and H_2 concentration in converted dry feed (3, 4) for CH_4 steam reforming on nanocomposite $Pt/Pr_{0.3}Ce_{0.35}Zr_{0.35}O_2$/Ni/YSZ layers supported on one side of Jülich Ni/YSZ anode platelet (1, 3) or porous Ni–Al substrate (2, 4). $CH_4/H_2O/Ar$ = 20/20/60. Contact time 25 ms.

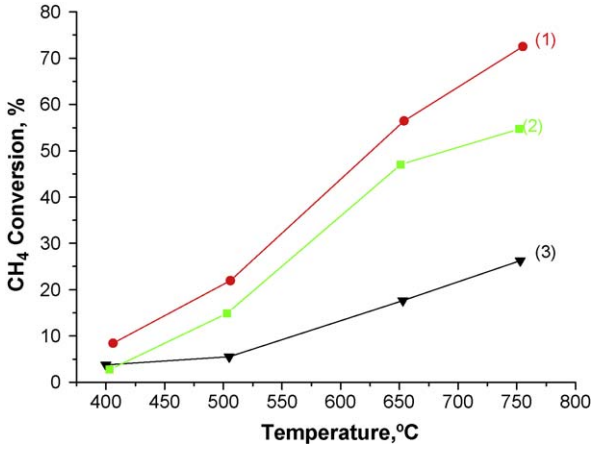

Fig. 9. Temperature dependence of CH_4 conversion for layers of 0.8 wt.% Ru/$La_{0.8}Pr_{0.2}Mn_{0.2}Cr_{0.8}O_3$/Ni/YSZ (1) or 0.39 wt.% Pt/$Pr_{0.3}Ce_{0.35}Zr_{0.35}O_2$Ni/YSZ (2) nanocomposites supported on one side of thin (0.8 mm) ECN porous anode substrate; (3) performance of pure porous ECN substrate. Feed 20% CH_4 + 20% H_2O in Ar, contact time 12 ms.

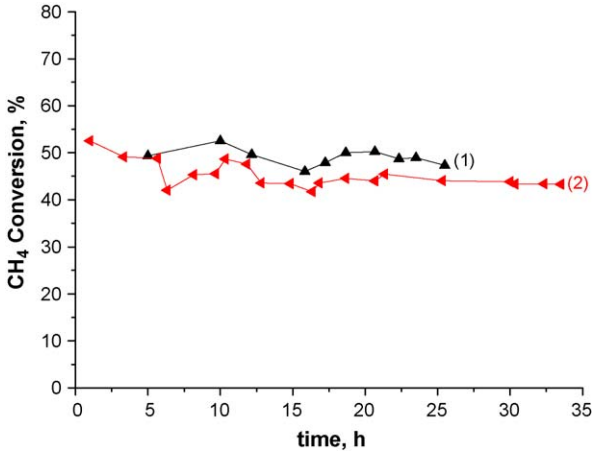

Fig. 10. Stability tests of thick (2 mm) FRZ Jülich anode platelet covered by Pt/$Pr_{0.3}Ce_{0.35}Zr_{0.35}O_2$ Ni/YSZ layer (1) or without it (2). Feed 20% CH_4 + 20% H_2O in Ar, contact time 24 ms, 650 °C.

deactivated in feeds with the steam excess were excluded from the list of promising systems, while composites promoted by Pt or Ru able to efficiently operate under a broad variation of the steam excess in the feed were selected for further application.

In addition to the direct in-cell steam reforming of methane occurring on catalytically active anodes of SOFC, nanocomposite catalysts supported on heat-conducting substrates such as Crofer interconnects or foam Ni–Al alloy can be efficiently applied for so-called indirect in-cell steam reforming of methane within the anode compartment of a stack (in fuel channels etc.) [3,4]. In this case, the effect of the oxygen transfer across the cell under load is of much less importance, so selection of active components can be primary oriented on achieving the highest performance in feeds with steam/methane ratio close to stoichiometry.

3.4. Catalytic performance of monolithic catalysts with supported nanocomposite active components in steam/autothermal reforming of oxygenates

Figs. 12 and 13 present preliminary results of pilot tests of monolithic catalysts with nanocomposite active component supported on heat-conducting Cr–Al composite substrates. Performance was reasonably stable at least for several hours yielding high concentration of syngas at rather short contact times for both types of active components even in feeds with relatively low H_2O content. H_2/CO ratio in syngas is close to 2 as expected by stoichiometry of the high-temperature reforming reaction. Main by-product is methane produced by the ethanol cracking. Addition of Ni into the active component helps to increase the yield of hydrogen and CO by decreasing methane content in the exit gas.

Fig. 14 presents results of the steam/oxysteam reforming of acetone on a monolithic catalyst in the pilot-scale reactor. For the active component comprised Pt + Ni-promoted complex fluorite-like oxide, a stable performance was achieved even in feeds without or with a small amount of added oxygen, thus implying small (if any) coking. However, some increase of syngas yield due to the oxygen addition suggests more efficient transformation of by-products (acetaldehyde etc) in more oxidizing conditions. In this case, the main by-product is also methane present in reasonably small amounts. In general, the yields of products are rather close to the stoichiometry of acetone reforming reactions in conditions of its complete transformation.

More detailed analysis of results of these experiments with a due regard for the temperature gradient in the monolith catalyst is beyond the scope of this paper and will be given elsewhere. However, it can be concluded that approach to design of stable to coking nanocomposite active components of methane steam reforming catalysts comprised complex oxides with a high lattice oxygen mobility along with combination of Ni with precious metals as components with a high efficiency in activation of fuel molecules is also quite efficient for design of catalysts for the reactions of oxygenates transformation into syngas.

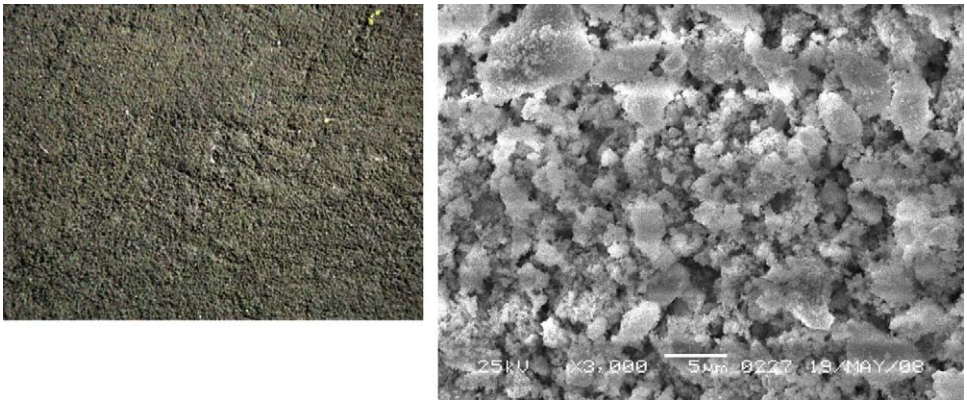

Fig. 11. Optical image (left, ×50) and SEM image (right) of FRZ Jülich anode platelet with supported nanocomposite layer after stability tests.

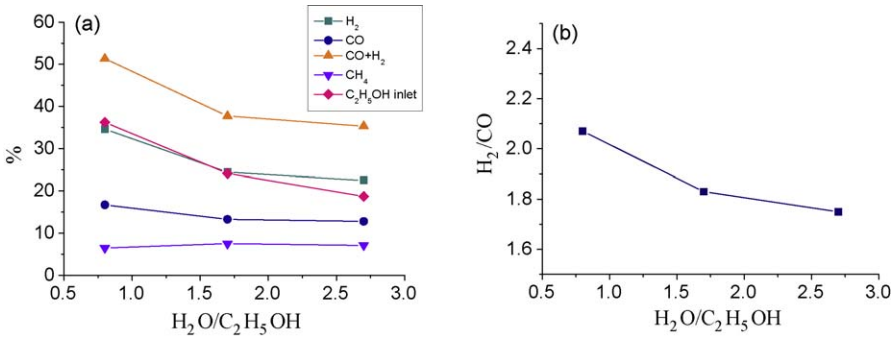

Fig. 12. Inlet concentration of ethanol and concentration of products in converted feed (a) and H_2/CO ratio in products (b) in ethanol steam reforming on monolithic Ru/(PrCeSmZr)O_2/Cr–Al composite catalysts. Contact time 0.02 s, monolith outlet temperature 860 °C, feed ethanol + H_2O + N_2 balance.

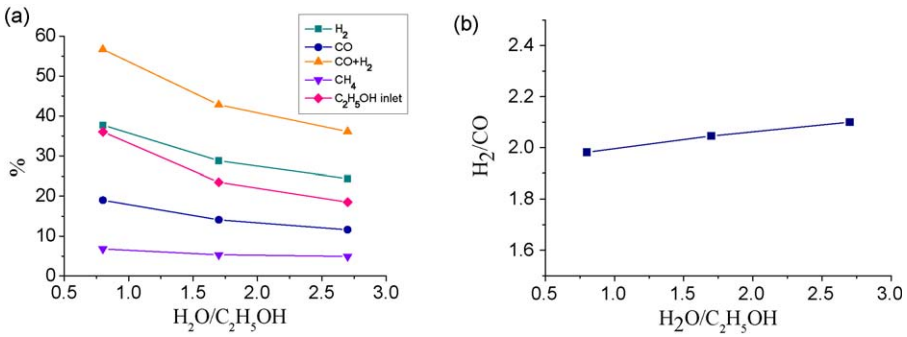

Fig. 13. Inlet concentration of ethanol, concentration of products in converted feed (a) and H_2/CO ratio in products (b) in ethanol steam reforming on monolithic Ru/(PrCeSmZr)O_2 + 10 wt.% NiO + 10 wt.% YSZ/Cr–Al composite catalysts. Contact time 0.02 s, monolith outlet temperature T_{outlet} 860 °C, feed ethanol + H_2O + N_2 balance.

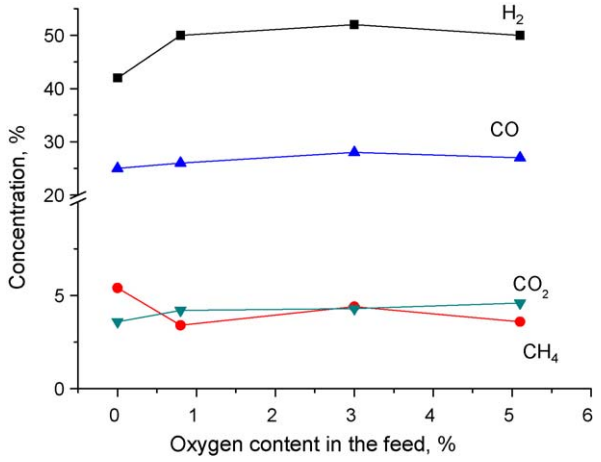

Fig. 14. Effect of O_2 content in the feed on concentration of products of acetone steam/oxysteam reforming on monolithic catalyst (Pt/Ni/La–Ce–Zr–O nanocomposite active component on monolithic thin-wall corundum substrate). Inlet feed composition: 24% acetone, 48% H_2O, 0–5% O_2, N_2 balance, feed inlet temperature 110 °C. Contact time 0.13 s, monolith outlet temperature T_{outlet} 850 °C.

4. Conclusions

Nanocomposites based upon Ni-doped zirconia anode materials co-promoted by perovskite-like or fluorite-like complex oxides and Pt group metals are efficient and stable to coking catalysts for in-cell steam reforming of methane required for IT SOFC design. Specificity of the catalytic properties of these materials with a due regard for the data of CH_4 TPR and H_2O TPO experiments is satisfactorily explained by the reaction scheme involving activation of CH_4 molecules on the surface of Ni particles promoted by precious metals while oxide components provide activation of water molecules and transfer of hydroxyls and/or hydroxocarbonate/oxygen species to the metal particles–oxide interface where they interact with activated C–H–O species producing syngas. This scheme explains strong effect of the catalysts composition and preparation procedure determining degree of interaction between components on activity and coking stability of these materials. The best combinations include as co-promoters Pt with fluorite-like oxides and Ru with perovskite-like oxides. Procedures for supporting thin layers of nanocomposite active components on different substrates including Ni/YSZ anode platelets, refractory dense/porous metal alloys, cermet or corundum monolithic carriers were developed. These structured catalysts demonstrated a high efficiency and stability in the reactions of steam reforming of methane as well as oxygenates (ethanol, acetone) in pilot-scale reactors.

Acknowledgements

Support of different parts of this work by EC FP6 SOFC 600, NATO SFP 980878, INTAS 05-1000005-7663, INTAS YSF 06-1000014-5773 Projects and Integration Project 57 of SB RAS-Belorussian Academy of Sciences is gratefully acknowledged.

References

[1] S. Primdahl, M. Mogensen, Solid State Ionics 152–153 (2002) 597.
[2] A. Atkinson, S. Barnett, R. Gorte, J. Irvine, A. Mcevoy, M. Mogensen, C.S. Singhal, J. Vohs, Nature 3 (2004) 17.
[3] K. Wincewicz, J. Cooper, J. Power Sources 140 (2005) 280.
[4] A. Dicks, J. Power Sources 71 (1998) 111.
[5] W. Jamsak, S. Assabumrungrat, P.L. Douglas, N. Laosiripojana, R. Suwanwarangkul, S. Charojrochkul, E. Croiset, Chem. Eng. J. 133 (2007) 187.
[6] M.C.J. Bradford, M.A. Vannice, J. Catal. 173 (1998) 157.

[7] M.M.V.M. Souza, M. Schmal, Appl. Catal. A: Gen. 255 (2003) 83.
[8] V. Sadykov, N. Mezentseva, R. Bunina, G. Alikina, A. Lukashevich, V. Rogov, E. Moroz, V. Zaikovskii, A. Ishchenko, O. Bobrenok, A. Smirnova, J. Irvine, O. Vasylyev, Mater. Res. Soc. Symp. Proc. 972 (2007), AA03.06.
[9] V.A. Sadykov, N.V. Mezentseva, R.V. Bunina, G.M. Alikina, A.I. Lukashevich, T.S. Kharlamova, V.A. Rogov, V.I. Zaikovskii, A.V. Ishchenko, T.A. Krieger, O.F. Bobrenok, A. Smirnova, J. Irvine, O.D. Vasylyev, Catal. Today 131 (2008) 226.
[10] V. Sadykov, N. Mezentseva, G. Alikina, R. Bunina, V. Rogov, T. Krieger, S. Belochapkine, J. Ross, Catal. Today 145 (2009) 127–137.
[11] V.A. Sadykov, N.V. Mezentseva, R.V. Bunina, G.M. Alikina, A.I. Lukashevich, V.I. Zaikovskii, O.F. Bobrenok, J. Irvine, O.D. Vasylyev, A.L. Smirnova, J. Fuel Cell Sci. Technol., in press.
[12] V.A. Sadykov, S.N. Pavlova, R.V. Bunina, G.M. Alikina, S.F. Tikhov, T.G. Kuznetsova, Yu.V. Frolova, A.I. Lukashevich, O.I. Snegurenko, N.N. Sazonova, E.V. Kazantseva, Yu.N. Dyatlova, V.V. Usol'tsev, I.A. Zolotarskii, L.N. Bobrova, V.A. Kuz'min, L.L. Gogin, Z.Yu. Vostrikov, Yu.V. Potapova, V.S. Muzykantov, E.A. Paukshtis, E.B. Burgina, V.A. Rogov, V.A. Sobyanin, V.N. Parmon, Kinet. Catal. 46 (2005) 227.
[13] A. Smirnova, V. Sadykov, V. Muzykantov, N. Mezentseva, V. Ivanov, V. Zaikovskii, A. Ishchenko, N. Sammes, O. Vasylyev, J. Kilner, J. Irvine, V. Vereschak, I. Kosacki, N. Uvarov, V. Zyryanov, Mater. Res. Soc. Symp. Proc. 972 (2007), AA10.05.
[14] V. Sadykov, S. Pavlova, O. Snegurenko, Z. Vostrikov, S. Tikhov, V. Kuzmin, V. Parmon, V. Ulianitskii, O. Brizitskii, A. Khristolyubov, V. Terentiev, Stud. Surf. Sci. Catal. 172 (2007) 241.
[15] S.F. Tikhov, V.V. Usoltsev, V.A. Sadykov, S.N. Pavlova, O.I. Snegurenko, L.L. Gogin, Z.Yu. Vostrikov, A.N. Salanov, S.V. Tsybulya, G.S. Litvak, G.V. Golubkova, O.I. Lomovskii, Stud. Surf. Sci. Catal. 162 (2006) 641.
[16] S. Pavlova, S. Tikhov, V. Sadykov, Y. Dyatlova, O. Snegurenko, V. Rogov, Z. Vostrikov, I. Zolotarskii, V. Kuzmin, S. Tsybulya, Stud. Surf. Sci. Catal. 147 (2004) 223.
[17] J. Wei, E. Iglesia, J. Phys. Chem. B 108 (2004) 4094.
[18] V. Sadykov, Yu. Frolova-Borchert, N. Mezentseva, G. Alikina, A. Lukashevich, E. Paukshtis, V. Muzykantov, L. Batuev, T. Kuznetsova, E. Moroz, D. Zyuzin, V. Kol'ko, E. Burgina, V. Kriventsov, D. Kochubei, E. Kemnitz, K. Scheurell, Mater. Res. Soc. Symp. Proc. 900E (2006), O10.08.
[19] V.A. Sadykov, N. Mezentseva, G. Alikina, A. Lukashevich, V. Muzykantov, T. Kuznetsova, L. Batuev, M. Fedotov, E. Moroz, D. Zyuzin, V. Kolko, V. Kriventsov, V. Ivanov, A. Boronin, E. Pazhetnov, V. Zaikovskii, A. Ishchenko, V. Rogov, J. Ross, E. Kemnitz, Mater. Res. Soc. Symp. Proc. 988 (2007), QQ06.04.
[20] V.A. Sadykov, N.V. Mezentseva, G.M. Alikina, A.I. Lukashevich, Yu.V. Borchert, T.G. Kuznetsova, V.P. Ivanov, S.N. Trukhan, E.A. Paukshtis, V.S. Muzykantov, V.L. Kuznetsov, V.A. Rogov, J. Ross, E. Kemnitz, K. Sheurell, Solid State Phenom. 128 (2007) 239.
[21] A. Sauvet, J. Irvine, Solid State Ionics 167 (2004) 1.